to be integrated, with appropriate weight for reliability of the forecast, with models of impact and logistics which require detailed information on infrastructure, population and other parameters over the location. Such models, which are necessarily location-specific, are in their infancy, especially in India.

1. James, M. K., Urban metabolism and disaster vulnerability in an era. In *Earth System Analysis* (eds Schellnhuber, H.-J. and Wenzel, V.), Springer-Verlag, Berlin, 1998, pp. 359–377.
2. Gilbet, A. and Gugler, J., *Cities, Poverty and Development: Urbanization in the Third World*, Oxford University Press, Oxford, 1992.
3. Jones, B. and Kandell, W. A., Population growth, urbanization, disaster risk and vulnerability in metropolitan areas: A conceptual framework. In *Environmental Management and Urban Vulnerability* (eds Kreimer, A. and Munasinghe, M.), World Bank Discussion Paper 168, 1992, pp. 51–76.
4. De, U. S., Dube, R. K. and Prakasa Rao, G. S., Extreme weather events over India in the last 100 years. *J. Indian Geophys. Union*, 2005, **9**, 173–187.
5. Haylock, M. and Nicholas, N., Trends in extreme rainfall indices for an updated high quality data set for Australia, 1910–1998. *Int. J. Climatol.*, 2000, **20**, 1533–1541.
6. Parker, M. D. and Johnson, R. H., Organizational modes of midlatitude mesoscale convective systems. *Mon. Weather Rev.*, 2000, **128**, 3413–3435.
7. Xie, P. and Arkin, P. A., Analyses of global monthly precipitation using gauge observations, satellite estimates and numerical model predictions. *J. Climate*, 1996, **9**, 840–858.
8. Pingping, X., Yarosh, Y., Love, T., Janowaik, J. E. and Arkin, P. A., A real-time precipitation analysis over South Asia. AMS Meeting, USA, 2002, 3.15–3.16.
9. Kisstler, R. *et al.*, The NCEP–NCAR 50-year Reanalysis: Monthly means CD-ROM and documentation. *Bull. Am. Meteorol. Soc.*, 2001, **82**, 247–267.
10. Rajeevan, M., Bhate, J., Kale, J. D. and Lal, B., Development of high resolution daily gridded rainfall data for the Indian region, India Meteorological Department. *Meteorol. Monograph Climatology*, 22/2005, 1–26.
11. Tamguay, M., Bartello, P. and Gauthier, P., Four dimensional data assimilation with a wide range of scales. *Tellus B*, 1995, **47**, 974–997.
12. Goswami, P. and Patra, G. K., Characteristic scale of convective organization and monsoon intensity. *Geophys. Res. Lett.*, 2004, **31**, L24109.
13. Ramesh, K. V. and Goswami, P., Reduction in temporal and spatial extent of the Indian summer monsoon. *Geophys. Res. Lett.*, 2007, **34**, L23704.
14. Palmer, T. N. and Raisanen, J., Quantifying the risk of extreme seasonal precipitation events in a changing climate. *Nature*, 2002, **415**, 512–514.
15. Schnur, R., The investment forecast. *Nature*, 2002, **415**, 483–484.
16. James, M. K. and Ericksen, N., Effects of climate changes on weather-related disasters. In *Confronting Climate Change: Risks, Implications and Responses* (ed. Mintzer, I.), Cambridge University Press, Cambridge. 1992, pp 141–152.
17. Mohanty, U. C. *et al.*, Weather summary during pilot experiment of severe thunderstorms – Observations and regional modelling (STORM), DST Report, 2006, pp. 1–146.

ACKNOWLEDGEMENTS. We thank Pingping Xie, NOAA/Climate Prediction Centre, USA for providing information about the high-resolution satellite-derived rainfall data over the South Asian region. This work was partially supported by a research grant from CSIR, New Delhi.

Received 20 March 2007; revised accepted 10 March 2008

Impact of ice-albedo feedback on hemispheric scale sea-ice melting rates in the Antarctic using Multi-frequency Scanning Microwave Radiometer data

Amitabh Mitra[1], I. M. L. Das[1,2,*], Mihir Kumar Dash[3], S. M. Bhandari[4] and N. K. Vyas[4]

[1]K. Banerjee Centre of Atmospheric and Ocean Studies,
[2]Department of Physics, University of Allahabad,
Allahabad 211 002, India
[3]Centre for Oceans, Rivers, Atmosphere and Land Sciences,
Indian Institute of Technology, Kharagpur 721 302, India
[4]Space Applications Centre, Indian Space Research Organization,
Ahmedabad 380 015, India

The sea-ice cover in the polar regions is one of the most expansive and seasonal geophysical parameters on the earth's surface. The presence or absence of sea-ice affects the atmosphere and the ocean, and therefore the climate in many ways. In this study we have used the Multi-frequency Scanning Microwave Radiometer (MSMR) brightness temperature data over the Antarctic/Southern Ocean region to calculate the weekly sea-ice extents, during the melting phase from August 1999 to March 2000 to quantitatively estimate the melting rates of sea-ice on a hemispheric scale. Compared to the melting rates based on the seasonal cycle of the solar irradiance, the MSMR-estimated melting rate remains less until the beginning of October and then rapidly increases to its peak value by the end of December. The observed melting rate behaviour indicates that apart from the seasonal cycle of solar irradiance, it is controlled by other mechanisms like the ice-albedo feedback. The present study estimates the feedback factor, response time and acceleration in the melting rate, which are important towards a better quantitative understanding of the future of Antarctic sea-ice variability, and the climate trends in the context of global warming.

Keywords: Hemispheric scale, ice-albedo feedback, melting rate, sea-ice extent.

IN the polar regions, sea water freezes at the surface due to the seasonal cycle of insolation producing a thin and discontinuous blanket of ice called sea-ice, having thickness of less than a few metres. The sea-ice acts as an efficient barrier to the free exchange of heat, moisture, and momentum fluxes between the ocean and the atmosphere, substantially altering the radiative and turbulent components of the surface-heat balance. Since the sea-ice layer is thin, its areal extent and thickness respond rapidly to changes in the surface heat balance and modulate the in-

*For correspondence. (e-mail: profimldas@yahoo.com)

teractions between the atmosphere and ocean on timescales extending from days to months and years. The thickness and areal extent of sea-ice has a major influence on the state of the ocean and the atmosphere. They appear to play a key role in the weather and climate and are important components of research into the past, present and future of the earth's climate system[1]. Sea-ice growth and melting are major factors in controlling the seasonal cycle of the air temperature and the upper ocean salinity in the polar regions. Sea-ice influences the climate through various feedback mechanisms. The most important feedback mechanism is the albedo-temperature feedback: an initial small warming (cooling) implies a decrease (increase) in the sea-ice extent and, hence a smaller (larger) reflection and larger (smaller) absorption of total incident solar energy over the region, which would be conducive to further enhancement of the initial warming (cooling). The mean albedo (α) of sea-ice ranges roughly from 0.5 to 0.7, compared to 0.05–0.15 for the open water[2,3]. As a result of the high albedo of ice surfaces, only a small fraction ($1 - \alpha$) of the energy is absorbed at the surface. Solar heating of the surface during summer results in the increase of snow/ice wetness and development of melt ponds, which in turn, significantly reduce the regionally averaged summer-time albedo[4]. This reduction in albedo plays an important role in the polar regions. Any perturbation in the surface energy balance resulting in a decrease of ice extent due to warming may spread and amplify, since the reduction of ice extent, in turn, increases the amount of solar energy absorbed by the system[5]. Another feedback mechanism is provided by sea-ice modifying the evaporation rates: a decrease (increase) in the sea-ice compactness through melting (freezing) leads to higher (lower) water vapour concentration in the lower atmosphere and to an enhancement (inhibition) of the atmospheric longwave radiative absorption, thus supporting further ice ablation (accretion). Because of such feedback effects between the surface and the atmosphere, the climate change signals are expected to be amplified in the polar regions[6].

Large expanses of remote areas in the polar regions pose several challenges in collecting *in situ* data. The visible sensors have limited capability for remote sensing of polar regions due to prolonged periods of darkness and cloud cover. Passive microwave remote sensing provides an alternative means for data acquisition and monitoring of the polar regions[7], because of the day and night capability of microwaves to penetrate the clouds in all-weather conditions.

Passive microwave remote sensing has been used for over 30 years to detect and monitor changes in sea-ice over the polar region[8]. Here the sensor detects the natural emission from the earth's surface, near surface, and the atmosphere. The intensity of microwave radiation, thermally emitted by an object is usually expressed in terms of brightness temperature T_B, which is the product of the emissivity and the physical temperature of the object, because of the proportionality of the microwave radiation with the latter.

Indian Remote Sensing Satellite (IRS-P4) was launched in a near polar orbit on 26 May 1999 from the indigenously developed Polar Satellite Launch Vehicle (PSLV). It was later renamed as Oceansat-1. It carried two payloads: (i) the Ocean Colour Monitor (OCM), mainly for biological remote sensing of oceans and (ii) the Multifrequency Scanning Microwave Radiometer (MSMR) to study the physical parametres of the ocean and the overlying atmosphere. The MSMR collects data in four microwave channels at frequencies 6.6, 10.65, 18 and 21 GHz for both vertical (V) and horizontal (H) polarizations. It provides the coverage of the whole earth except for a small region around the poles, with a repeat cycle of once in 2 days. The MSMR brightness temperature daily data at 18 GHz (H) channel has been used for the present study, from 22 August 1999 to 22 March 2000, over the Antarctic region, during which the sea-ice is in its melting phase. The 18 GHz (H) channel was chosen because of (a) higher spatial resolution of 50 km compared to 6 and 10.65 GHz channels (which have resolutions of 150 and 75 km respectively), (b) lesser influence of water vapour compared to 21 GHz channels and (c) better distinction of sea-ice features compared to 18 GHz (V) channel[9]. Microwave emission comes from different layers such as the snow surface, snow–ice interface and the internal ice layers, and depends on the frequency. Open water is reflective in the microwave band and emits little energy, and has strong polarization. In contrast, first-year ice is highly emissive and has weak polarization, while the multiyear ice emission falls between that of water and the first-year ice. Consequently, the brightness temperature recorded by the sensor depends on the type of surface from which the radiation has emanated. The optimum and round-the-year boundary for distinguishing the sea-ice from open water in the Antarctic using the MSMR 18 GHz (H) channel data was found[9] to be at $T_B > 130$ K. Any values above this threshold represent sea-ice and those below represent open water. Weekly average (6–8 days) brightness temperature data files were prepared on a $0.5° \times 0.5°$ latitude–longitude grid for the study period, starting from 22–27 August 1999 up to 15–22 March 2000. The weekly brightness temperature data were then displayed in image form using Grads software in polar stereographic projection from 50°S to 90°S with a properly chosen scale for each of the plots. Figure 1 *a* and *b* shows the typical weekly average brightness temperature plots obtained in this way during the winter of 1999 and the summer of 2000. Then the weekly sea-ice extents were calculated. Here sea-ice extent refers to the area covered by sea-ice from the continental boundary to the ice edge in the open ocean. Etopo file obtained from USGS was used to define the continental boundary of Antarctica. Details of MSMR data and analysis are presented elsewhere[10]. MSMR data have

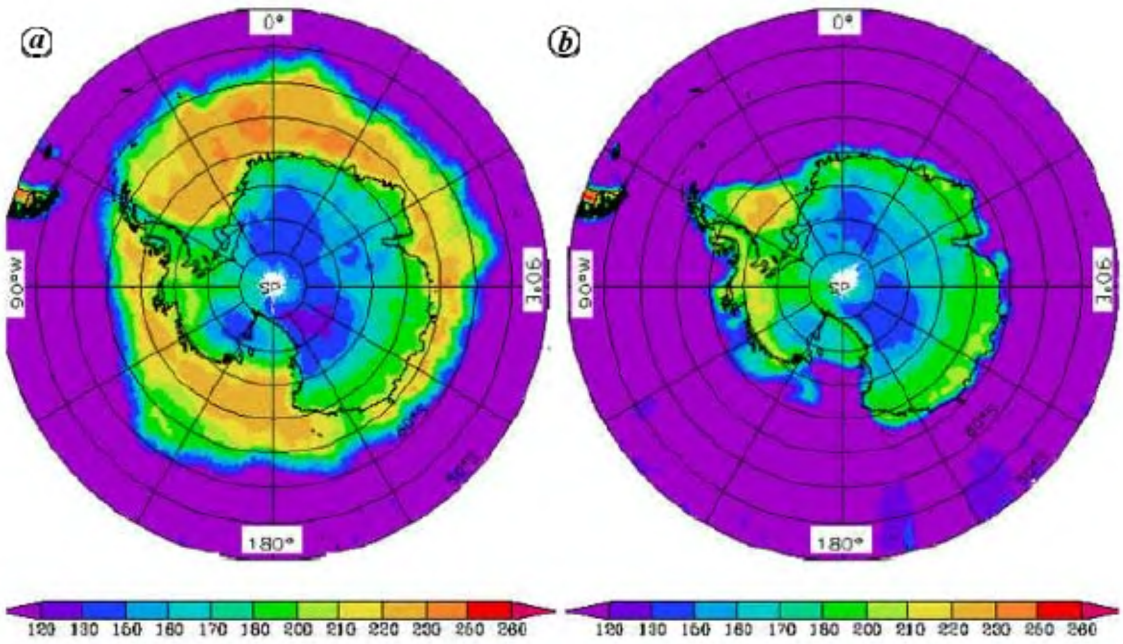

Figure 1. Brightness temperature map (*K*) obtained from MSMR showing the sea-ice extent in Antarctica for (***a***) the week 22–27 August 1999 (southern winter) and (***b***) the week 22–27 February 2000 (southern summer).

been used earlier to study the north–south migration of sea-ice edge around Antarctica[11].

Weekly sea-ice extents were calculated from 22–27 August 1999 to 15–22 March 2000, using the MSMR brightness temperature data and the melting rate derived from the MSMR observed data, corresponding to the mid-day of each week. The mid-day of the first week (24 August 1999) was allocated the time $t = 0$, and it also corresponds to the maximum sea-ice area during the study period. Then, $t = 184$ (almost equal to half of a leap year of 366 days) corresponds to the mid-day of the week 22–27 February 2000 (24 February 2000), and it is almost coinciding with the minimum sea-ice area during the period of our study.

We fit a cosine curve of the form given by eq. (1) for the sea-ice extent values against time t in days, during the melting phase:

$$Y = c + a\cos(\omega t), \tag{1}$$

where Y represents the expected sea-ice extent. Here $\omega = 2\pi/T$, where $T = 365.24$ days, corresponding to a periodicity of one year. The cosine curve is chosen for the fitting purpose in view of the fact that the solar irradiance at a given latitude depends on the seasonal variation of the cosine of the solar elevation angle at that latitude during the apparent annual motion of the sun along the ecliptic. For $t = 0$ (i.e. on 24 August 1999), the sea-ice extent value $Y = 21.86547$ million km^2 was maximum and for $t = 184$ (i.e. on 24 February 2000), the sea-ice extent value $Y = 4.78273$ million km^2 was almost minimum. Using these two conditions, the coefficients in eq. (1) were determined as $a = 8.54257$ and $c = 13.32290$, since $\cos(\omega t) = -0.99972$ at $t = 184$.

Figure 2 shows the observed sea-ice extent values derived from MSMR data and those expected from eq. (1). The two curves match closely in portions A and C, representing the start and end of the melting season respectively. However, we observed a systematic difference between the corresponding points of the two curves in the intermediate phase represented by part B of the curve. During the intermediate phase B, the observed sea-ice extent (Obs.) values were well above the expected values (Th.) based purely on the annual variation of the solar irradiance.

In Figure 2 the gradient of the MSMR observed sea ice extent curve (Obs.) appears to be less inclined at the start, but later it steepens and then gradually reduces until the peak of summer arrives. The possible cause of this phenomenon is that the existing sea-ice-albedo of the region resists the incoming solar radiation from melting the surface, thus keeping the melting rate low at the beginning. As the sea-ice starts melting, the open water fraction increases. The shortwave radiation over the open water fraction further increases the melt rate. This will lead to the formation of a steep gradient in the curve 'Obs.' in part B of the curve. This behaviour clearly illustrates the presence of the sea-ice-albedo – temperature feedback

process[12]. Finally, by the time the peak summer season arrives, the ablation rates become low again because little ice is left for melting.

The actual melting rate of sea-ice extent for each week was compared with the depletion rate obtained by differentiating eq. (1) as shown below

$$-(dY/dt) = a\omega \sin(\omega t). \quad (2)$$

Comparison of the actual melting rate of sea-ice extent with that obtained from eq. (2) is shown in Figure 3. The actual melting rate is less during the week 4–9 October 1999 at around day 43 and is equal to 0.02995 million sq. km per day, whereas the sea-ice extent is almost at its peak at 20.23562 million km^2. The melting rate picks up and reaches its peak during 22–27 December 1999 at around day 122 and is equal to 0.2155 million km^2 per day. Then the sea-ice extent starts decreasing rapidly and reaches its bare minimum (4.73696 million km^2) in the week 14–21 February 2000 at around day 177, with melting rate of only 0.00532 million km^2 per day. The peak melting rate derived from the observed data lags behind that obtained from eq. (2) based on the cycle of solar irradiance by nearly 30 days. This is perhaps because of the time taken by the melting process to complete in response to the absorbed solar radiation. It is evident from Figure 3 that during the melting phase, the actual rate of depletion of sea-ice extent remains low for a considerable time (from day 0 to 60) and then picks up and reaches a maximum (from day 60 to 120), and subsequently comes down at a steep rate (from day 120 to 160) and thereafter remains low. It deviates from the path expected purely from the cycle of solar irradiance described by eq. (2), suggesting the presence of some basic thermodynamic feedback processes controlling the extent of sea-ice.

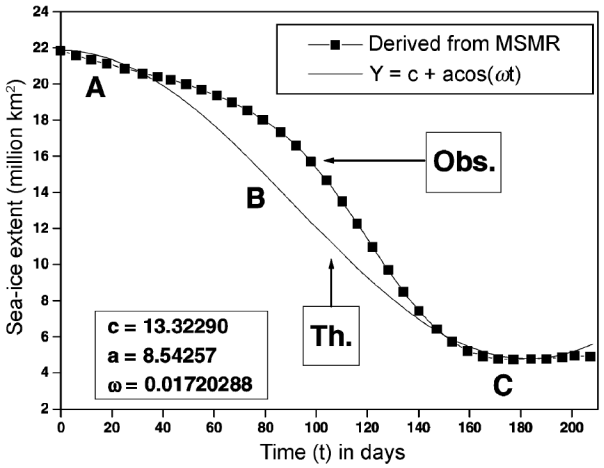

Figure 2. Weekly Antarctic sea-ice extents during the melting phase from 22 August 1999 to 22 March 2000.

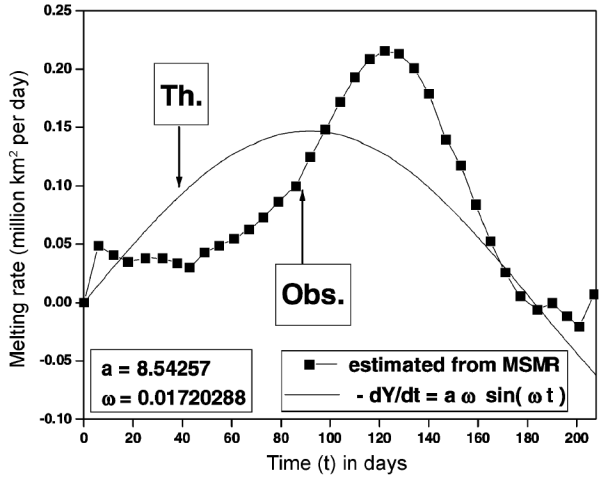

Figure 3. Weekly Antarctic sea-ice melting rates during the period 22 August 1999–22 March 2000.

The impact of these feedback processes is manifold (see Table 1; day numbers rounded to nearest 10). With the advancement of summer, the increasing solar radiation on the melting process gets moderated and a phase lag of about 60 days is introduced in the system. The whole system passes through an accelerated phase of melting with increasing melting rates for 60 days and decreasing melting rates for another 40 days. Effectively the melting is completed in about 100 days, which would have taken about 180 days in the absence of the feedback processes. Thus, the effective speed of melting gets amplified by a factor of 1.8 times. The peak melting rate of ~0.14 million km^2 per day obtained from eq. (2) also gets amplified by a factor of about 1.5 to ~0.21 million km^2 per day in the MSMR estimated melting rate curve (Figure 3) and occurs with a delay of 30 days.

The age and thickness of sea-ice present in different sectors of the Antarctic Ocean also play a role in increasing/decreasing the absorption of solar radiation, as the melting process proceeds with time. Attempts were made to fit polynomials of different degrees to the 'Obs.' curve. It is found that the nature of the observed melting rate curve cannot be aptly described by a polynomial and requires an appropriate functional form to define its variation with time.

In comparison to the expected melting rates the actual melting rates of sea-ice extent, derived from the MSMR data were initially slow, but subsequently become fast possibly due to some basic sea-ice thermodynamic feedback processes like the ice-albedo feedback, which is expected to be the dominant process due to the large difference between the reflective properties of ice and water. The feedback acts with a system response delay of ~60 days, increasing the effective melting rates by 1.8 times and results into a peak impact factor of about ~1.5 (Table 1). More aspects of the feedback need to be explored. Since the polynomial relationships are not able to describe the

Table 1. Impact of the feedback process obtained from Figure 3

Observation		Time taken	Remarks
Very low melting rates	From day 0 to 60	60 days	Response time lag: 60 days
Accelerating melting rates	From day 60 to 120	60 days	Feedback process active
Decelerating melting rates	From day 120 to 160	40 days	Less ice left for melting
Low melting rates in the final phase	From day 160 onwards	20 days till day 180	Very little ice left and highly reduced solar insolation due to winter
Effective melting phase	From day 60 to 160	100 days, instead of 180 days of total summer	Acceleration of the effective melting rate 1.8 times, thereby reducing the effective melting period
Peak melting rate on the 'Obs.' curve	0.2155×10^6 km^2 per day	On day 122	With a delay of 30 days from the theoretically expected day 92
Peak melting rate on the 'Th.' curve	0.146946×10^6 km^2 per day	On day 92	
Feedback factor for the peak melting rate	Feedback impact factor of ~0.21/0.14 = 1.5		With a response time lag of 30 days

melt rate behaviour properly, we need a theoretical relationship that would describe the cryospheric feedback processes in a mathematical form. In any case, the amount of pre-existing sea-ice is an important component in determining the prevailing melting rates. It is, therefore, necessary to measure the sea-ice extents accurately in the present climate to better understand the future of Antarctic sea-ice variability[13].

In conclusion, the satellite-estimated melting rates clearly bring out the impact of the cryospheric feedback processes that control and dominate the seasonal melting rates of sea ice.

1. Thomas, D. N. and Dieckmann, G. S., *Sea Ice: An Introduction to its Physics, Chemistry, Biology and Geology*, Blackwell Publishing, 2003, p. 6.
2. Grenfell, T. C. and Maykut, G. A., The optical properties of ice and snow in the Arctic Basin. *J. Glaciol.*, 1977, **18**, 445–463.
3. Massom, R. and Comiso, J. C., The classification of Arctic sea ice types and the determination of surface temperature using advanced very high resolution radiometer data. *J. Geophys. Res.*, 1994, **99**, 5201–5218.
4. Eicken, H., Krouse, H. R., Kadko, D. and Perovich, D. K., Tracer studies of pathways and rates of meltwater transport through Arctic summer sea ice. *J. Geophys. Res.*, 2002, **107**.
5. Curry, J. A., Schramm, J. L. and Ebert, E. E., Sea ice-albedo climate feedback mechanism. *J. Climate*, 1995, **8**, 240–247.
6. Budyko, M. I., Polar ice and climate. In Proceedings of the Symposium on the Arctic Heat Budget and Atmospheric Circulation (ed. Fletcher, J. O.), RM 5233-NSF, Rand Corporation, Santa Monica, California, 1966, pp. 3–32.
7. Harouche, I. P.-F. and Barber, D. G., Seasonal characterization of microwave emissions from snow-covered first-year sea ice. *Hydrol. Process*, 2001, **15**, 3571–3583.
8. Parkinson, C. L. and Gloersen, P., Global sea ice coverage. In *Atlas of Satellite Observations Related to Global Change* (eds Gumey, R. J., Foster J. L. and Parkinson, C. L.), Cambridge University Press, Cambridge, 1993, pp. 371–383.
9. Vyas, N. K., Bhandari, S. M., Dash, M. K., Pandey, P. C., Khare, N., Khanolkar, A. and Sharma, N., *An Atlas of Antarctic Sea Ice from Oceansat-1 MSMR*, A joint publication of NCAOR, Goa and SAC (ISRO), Ahmedabad, 2004, p. 7.
10. Bhandari, S. M., Vyas, N. K., Dash, M. K., Khanolkar, A., Sharma, N., Khare, N. and Pandey, P. C., Simultaneous MSMR and SSM/I observations and analysis of sea ice characteristics over the Antarctic region. *Int. J. Remote Sensing*, 2005, **26**, 3123–3136.
11. Bhandari, S. M., Vyas, N. K., Sharma, N., Dash, M. K., Khare, N. and Pandey, P. C., Remote sensing studies of the seasonally oscillating sea ice boundary over the Southern Polar Ocean around Antarctica using Oceansat-1 MSMR. In *Seminar on Earth Science of East Antarctica*, Geological Survey of India and the (Indian) National Centre for Antarctic and Ocean Research, New Delhi, 15–16 September 2005, p. 40.
12. Yao, T., Tang, C. L. and Peterson, I. K., Modeling the seasonal variation of sea ice in the Labrador Sea with a coupled multicategory ice model and the Princeton ocean model. *J. Geophys. Res.*, 2000, **105**, 1153–1165.
13. Vyas, N. K., Dash, M. K., Bhandari, S. M., Khare, N., Mitra, A. and Pandey, P. C., On the secular trend in sea ice extent over the Antarctic region based on OCEANSAT-1 MSMR observations. *Int. J. Remote Sensing*, 2003, **24**, 2277–2287.

ACKNOWLEDGEMENTS. A.M. and I.M.L.D. thank NCAOR, Goa/DOD for a research grant. We also thank Dr. A. Sarkar, Head, Ocean Sciences Division, SAC, Ahmedabad for encouragement during the course of this work.

Received 10 April 2007; revised accepted 26 February 2008